Kinetochore dynein: its dynamics and role in the transport of the Rough deal checkpoint protein

Edward Wojcik*†§, Renata Basto‡, Madeline Serr†, Frédéric Scaërou‡, Roger Karess‡ and Thomas Hays†

**Virginia Tech University, Department of Biology, Blacksburg, Virginia 24061, USA*
†Department of Genetics, Cell Biology, and Development, University of Minnesota, Minneapolis, Minnesota 55108, USA
‡C.N.R.S., Centre de Génétique Moleculaire, Avenue de la Terrasse, 91198 Gif-sur-Yvette, France
§e-mail: ewojcik@vt.edu

We describe the dynamics of kinetochore dynein–dynactin in living *Drosophila* embryos and examine the effect of mutant dynein on the metaphase checkpoint. A functional conjugate of dynamitin with green fluorescent protein accumulates rapidly at prometaphase kinetochores, and subsequently migrates off kinetochores towards the poles during late prometaphase and metaphase. This behaviour is seen for several metaphase checkpoint proteins, including Rough deal (Rod). In neuroblasts, hypomorphic dynein mutants accumulate in metaphase and block the normal redistribution of Rod from kinetochores to microtubules. By transporting checkpoint proteins away from correctly attached kinetochores, dynein might contribute to shutting off the metaphase checkpoint, allowing anaphase to ensue.

Genetic and biochemical analyses suggest that cytoplasmic dynein serves multiple functions during mitosis. For example, clear roles for dynein in spindle morphogenesis and centrosome attachment to the spindle have been observed[1–7]. In addition, experiments in several different systems implicate dynein in the regulation of spindle orientation and positioning[8–14]. Although still controversial, a closer inspection of kinetochore assembly and function is beginning to reveal roles for dynein in additional mitotic pathways.

The localization of cytoplasmic dynein to kinetochores fostered an early interest in dynein as a motor for movements from chromosome to pole[15,16]. Support for this hypothesis comes from two recent sets of experiments. First, aberrant polewards chromosome movements occur when *Drosophila* embryos are injected with a dynein heavy-chain antibody or heterologous mammalian p50/dynamitin (Dmn)[17]. Second, when recruitment of dynein to the kinetochore is perturbed or eliminated by mutations in *rough deal* (*rod*) and *zeste-white10* (*zw10*)[18,19], subsequent chromosome movements are also impaired. Interestingly, both Rod and Zw10 are components of the metaphase checkpoint[19–21]. Still other evidence also suggests that dynein might function in the metaphase checkpoint pathway (discussed in refs 22–24). Moreover, the localization of dynein at grasshopper kinetochores is sensitive to microtubule attachment, indicating a potential role in monitoring the attachment state of kinetochores[22]. To obtain a better understanding of the potential roles for dynein at the kinetochore, we investigated the relation between the distribution of dynein–dynactin, the distribution of Rod protein, and mitotic checkpoint function.

Results

Dynactin dynamics in live embryos: transient accumulation of conjugate of p50 and GFP at kinetochores during mitosis. The p50/Dmn subunit of dynactin is a key regulator of dynein function during mitosis. Previous studies have implicated p50 and dynactin in both the localization and function of dynein at kinetochores, as well as in the physical interaction between dynactin and the checkpoint component Zw10 (refs 17, 19, 25). To monitor the localization of dynein and dynactin during mitosis in the syncytial embryo, we used a carboxy-terminal fusion of green fluorescent protein to *Drosophila* p50/Dmn (Dmn–GFP) (see Methods). Dmn–GFP transgenic flies were recovered that expressed a functional Dmn–GFP fusion protein. A single copy of the Dmn–GFP transgene is easily maintained as a stock and therefore produces no obvious ill effects on viability or fertility. The frequency of hatching for Dmn–GFP embryos is ~98% of the normal hatching frequency observed for wild-type embryos (see Methods). Most significantly, the Dmn–GFP fusion protein incorporates into, and does not disrupt, the native dynactin complex (Fig. 1). In mammalian tissue

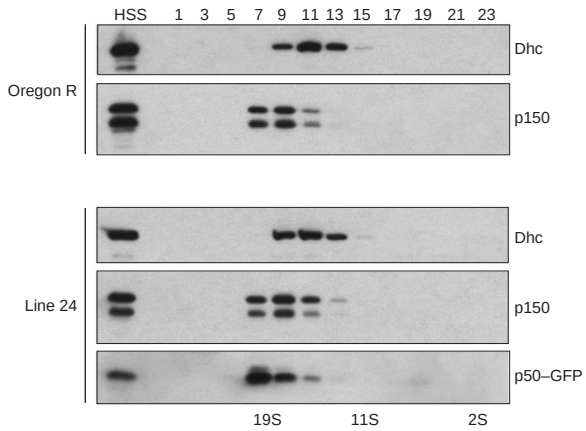

Figure 1 **p50/Dmn–GFP protein co-fractionates with the dynactin complex (19S) on a sucrose density gradient.** Potentially dissociated complexes arising from the expression of the Dmn–GFP transgene in wild-type animals are not detectable. Equal volumes of alternate fractions from 5–20% gradients were analysed by western blotting (see Methods). Fraction numbers are indicated above the appropriate lanes. HSS, initial soluble extract.

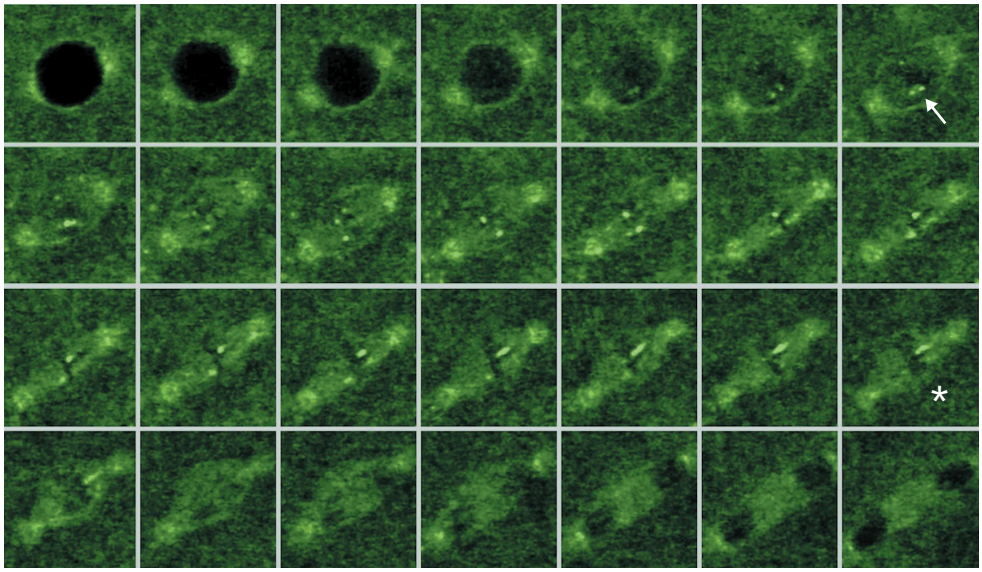

Figure 2 **Dmn–GFP dynamics in living embryos.** Shown are selected images from a time-lapse recording (see Supplementary Information) during mitosis in a syncytial embryo. Dmn–GFP/dynein accumulates rapidly at prometaphase kinetochores in high concentrations (an example is indicated by an arrow) and quickly translocates towards the spindle poles. As prometaphase and chromosome congression proceeds into anaphase (asterisk), the high levels of kinetochore dynein are gradually diminished. The individual frames of the figure are separated by 35 s each.

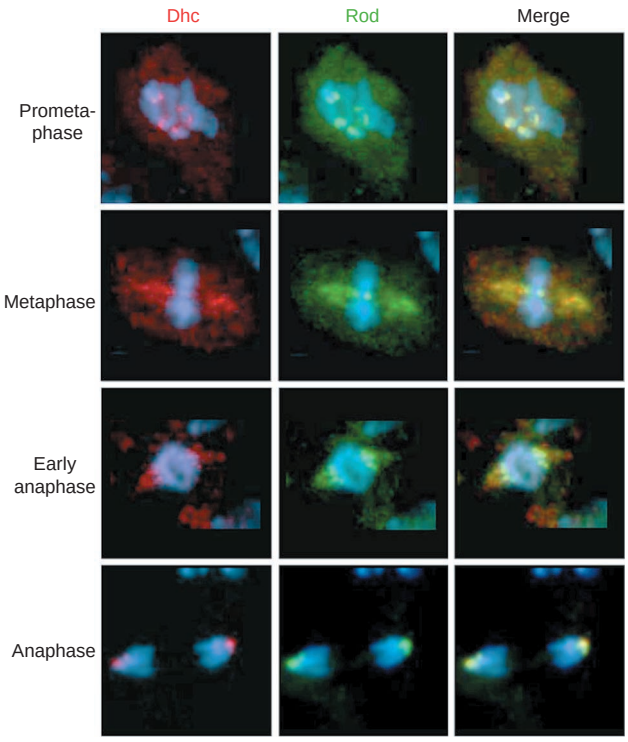

Figure 3 **Dynein and Rod colocalize during mitosis in *Drosophila* neuroblasts.** Shown are examples of immunolocalization of Rod (green), Dhc (red) and DNA (blue) in epifluorescence images taken from fixed, Triton-extracted third-instar larval neuroblasts. Note that both dynein and Rod redistribute along kinetochore microtubules during metaphase.

culture cells, severe overexpression of p50 disrupts the dynactin complex *in vivo* and alters mitotic chromosome behaviour[25]. Similarly, the injection of heterologous human p50 into *Drosophila* embryos at high concentration inhibits mitotic chromosome behaviour, but whether the dynactin complex is disrupted was not determined[17]. In our studies, Dmn–GFP transgene expression is under the control of the native Dmn promoter. Consequently, we attribute the observed stability of the native dynactin complex to the moderate level of Dmn–GFP expression and its normal incorporation into a functional dynactin complex.

The distribution of Dmn–GFP undergoes marked alterations during the embryonic mitotic cycles. Our analysis of nuclear cycles 10–14 shows that Dmn–GFP is enriched along the nuclear envelope of prophase nuclei and in the actin-rich cortex of the embryo (see Supplementary Information, Movie 1). Previously, an analysis of dynein mutants indicated that dynein is required for centrosome attachment and migration along the nuclear envelope[2]. The observed distribution of Dmn–GFP supports the hypothesis that dynactin might mediate dynein association with the nuclear envelope and thereby ensure proper centrosome migration during prophase.

During prometaphase, Dmn–GFP accumulates at both spindle poles and kinetochores. Whereas Dmn–GFP is detected at the spindle pole throughout mitosis, localization to the kinetochore is dynamic and transient. In early prometaphase, the Dmn–GFP signal can rapidly accumulate to high levels at individual kinetochores (Fig. 2, arrow). As prometaphase proceeds and the congression of chromosomes ensues, the Dmn–GFP signal at a kinetochore translocates towards the associated spindle pole. This polewards flux rapidly depletes the high levels of kinetochore Dmn–GFP observed in prometaphase to the invariably low but detectable levels present on metaphase and anaphase kinetochores (Fig. 2, asterisk). Although it has not been possible to monitor all kinetochores within a single spindle simultaneously, our analysis of time-lapse video recordings suggests that individual kinetochores behave independently with regard to the timing and level of Dmn–GFP accumulation. Given the well-established

association between the dynactin and dynein complexes[26], the visualization of the Dmn–GFP probably reflects the dynamics of both complexes. This inference is supported by recent observations made on fixed grasshopper spermatocytes that indicate similar dynamics for dynein at kinetochores[22].

The distribution of the checkpoint protein Rod during mitosis in *Drosophila* neuroblasts parallels that of kinetochore-associated cytoplasmic dynein (*Dhc64C*) and is dependent on dynein function. The prometaphase accumulation of Dmn–GFP at kinetochores is consistent with one or more roles for dynein in microtubule attachment, chromosome congression and/or checkpoint function. Dynein recruitment to kinetochores requires Rod and Zw10 (ref. 19), which are part of a complex functioning in the metaphase checkpoint[20,21,27]. To test whether dynein itself functions in the metaphase checkpoint, we examined the localization of dynein and Rod during mitosis in fixed detergent-extracted *Drosophila* larval neuroblasts (Fig. 3). We observed extensive coincidence in the localization of dynein and Rod at all stages of mitosis. Both proteins are prominent on prometaphase kinetochores and show a marked redistribution by metaphase. The complement of dynein and Rod on metaphase kinetochores declines significantly, while both proteins appear along the kinetochore microtubules and extend toward the attached spindle pole. This pattern of localization is consistent with the dynamic polewards flux of Dmn–GFP detected *in vivo* during the embryonic syncytial divisions and indicates a similar dynamic redistribution of both dynein and Rod in neuroblasts. These data suggest that dynein motor activity drives the redistribution of the Rod–Zw10 complex during mitosis. Interestingly, previous work has shown that Rod is involved in the recruitment of dynein to the kinetochore early in prometaphase[19]. Moreover, despite the polewards extension and progressive depletion of dynein from the kinetochore during prometaphase, there remain low but detectable levels of both Rod and dynamin heavy chain

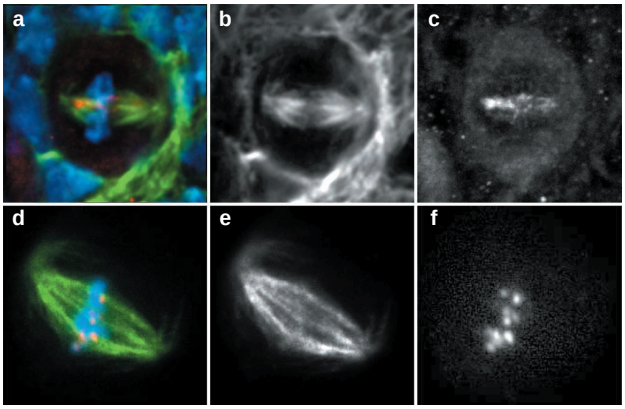

Figure 4 **Rod localization at metaphase is dependent on dynein function.** The top row shows a fixed wild-type third-instar metaphase larval neuroblast immunostained for Rod (red), tubulin (green) and DNA (blue). Rod has redistributed along the microtubules. By contrast, a *Dhc64C*$^{6-10}$ mutant metaphase neuroblast (bottom row) displays a strong kinetochore Rod signal and no microtubule signal, despite having achieved a well-formed spindle and metaphase plate. (**a**,**d**) Merged composite images of tubulin and Rod signals. The tubulin channels (**b**, **e**) and Rod channel (**c**, **f**) are shown separately for comparison.

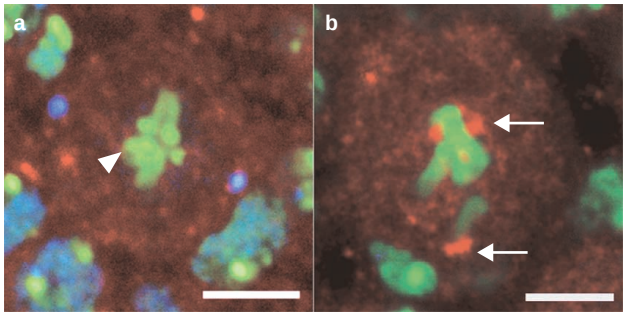

Figure 5 **Mutant dynein accumulates on kinetochores and does not spread polewards along kinetochore microtubules in metaphase third-instar giant neuroblasts. a**, Merged composite image of DNA (green), centrosome antigen CP190 (blue) and Dhc (red) in a fixed wild-type whole-mount preparation. The kinetochore/spindle signal for dynein at metaphase is typically low (arrowhead) and comparable to the general cytoplasmic signal in this type of preparation. **b**, By contrast, mutant Dhc (arrows: lower arrow points to a telocentric X chromosome) accumulates to high levels at kinetochores of *Dhc64C*$^{6-10}$*/Df(3L)10H* metaphase cells. Scale bar, 5 μm.

Table 1 Comparison of mitotic variables in wild-type and *Dhc*$^{6-10}$ mutant larval neuroblasts

	met/ana	Relative Mitotic index chromosomes	Overcondensed metaphsase	Polyploid metaphases	Abnormal anaphases	PSCS (%)
Wild type	2.9	1.0	1.3	0	4.6	1
Dhc$^{6-10}$*/Df(3L)10H*	9.2	1.6	17.5	7.0	29	1
Dhc$^{6-10}$, *rod*^{X6}	3.2	0.7	4.9	34	58	27

Polyploid metaphases, percentage of metaphase cells of apparent 4*N*, or greater, ploidy. In addition, a low incidence of ~2*N* aneuploid cells was observed (1-2 per brain, Figure 7). The frequency of aneuploidy seems lower than that observed for *rod* mutants[33].
Met/Ana, ratio of metaphase to anaphase figures from chromosome spreads of 10 animals (see below).
Mitotic index, ratio of total number of mitotic figures observed for 400 random wild-type microscope fields to an equal number of mutant fields. The fields were sampled equally from 10 animals from different experiments for both wild-type and mutant chromosome spreads.
Abnormal anaphases, any broad or disorganized arrays containing lagging chromosomes, including PSCS arrays.
PSCS, percentage of abnormal anaphases that show PSCS.
50±5 fields were counted per animal for 10 wild-type and *Dhc*$^{6-10}$ animals, respectively. This included over 1750 mitotic figures in WT and over 2700 mitotic figures in *Dhc6-10/Df(3L)10H* animals. 200 fields from 6 *Dhc*$^{6-10}$, *rod*^{X6} animals were tallied. Statistical significance was confirmed by the Mann–Whitney Rank Sum test

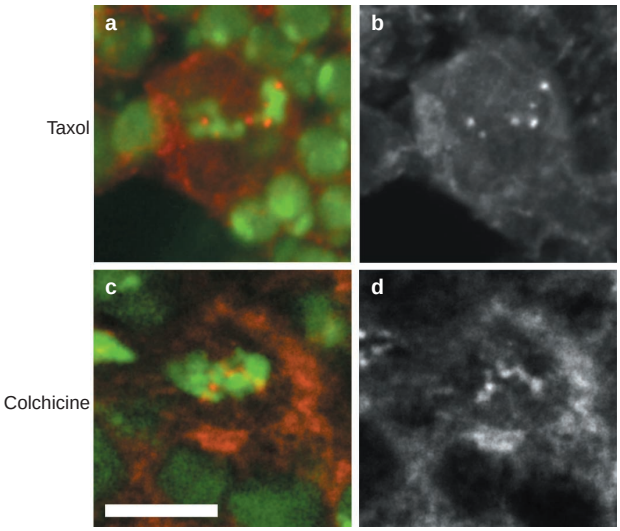

Figure 6 **Drugs that alter microtubule assembly and dynamics block polewards migration of dynein. a**, **c**, Confocal immunolocalization of DNA (green) and Dhc (red) within wild-type third-instar neuroblasts. The Dhc signals from **a** and **c** are shown separately in **b** and **d**, respectively. When metaphase mitotic spindles are disrupted by the action of either Taxol (**a**, **b**) or colchicine (**c**, **d**), Dhc is seen to accumulate abnormally at kinetochores similarly to mutant dynein (*Dhc64C*$^{6-10}$) alone (Fig. 3).

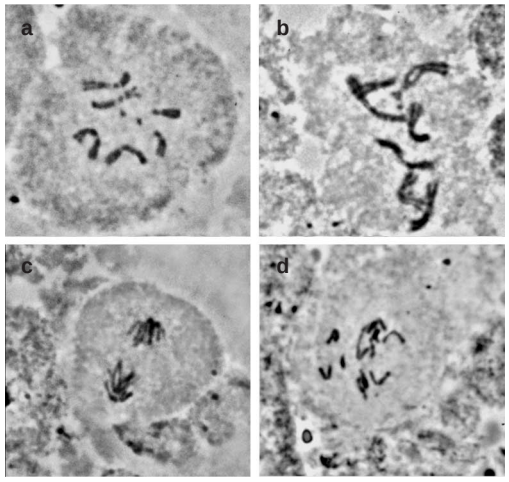

Figure 7 **Dynein mutant neuroblasts are delayed in metaphase and suffer mitotic defects, but do not exhibit premature sister chromatid separation.** When compared with the wild type (**a**, **c**), mutants (*Dhc64C*$^{6-10}$) showed relatively high frequencies of both aneuploid (**b**) and polyploid cells (not shown), as well as mitotic cells with abnormal anaphase configurations (**d**) (see also Table 1).

(Dhc) at the kinetochores throughout mitosis. The dynein retained at kinetochores might contribute to polewards chromosome movements[17,18].

If Rod behaviour depends in part on dynein function, then dynein mutations would be expected to influence Rod function. In the background of the strong hypomorphic cytoplasmic dynein allele, *Dhc64C*$^{6-10}$, we observed a marked effect on Rod localization (Fig. 4). In the *Dhc64C*$^{6-10}$ mutant cells, both the mutant Dhc and Rod products remain abundant at the kinetochores of chromosomes aligned on the metaphase plate. Both mutant products fail to redistribute along the kinetochore fibres (Fig. 4d–f), whereas in wild-type cells (Fig. 4a–c) Rod and Dhc are no longer prominent on metaphase kinetochores; instead, both are similarly localized along the entire length of the kinetochore spindle fibres.

When prepared without detergent extraction, the resulting high level of dynein in the cytoplasm of wild-type preparations masks the relatively weak kinetochore-associated dynein signal in metaphase neuroblasts. In contrast, under these conditions, mutant dynein (*Dhc64C*$^{6-10}$) is easily seen on metaphase kinetochores, suggesting that inappropriately high levels of dynein remain on metaphase kinetochores (Figs 5 (arrows) and 7a, b,). Thus, although the mutant Dhc is able to localize to the kinetochores, it seems unable to traffic off the kinetochore and out onto the kinetochore fibres. The correlated retention of Rod at kinetochores is consistent with the interpretation that dynein function mediates the depletion of Rod from the kinetochore and its redistribution along kinetochore microtubules during metaphase.

The dependence of Rod localization on dynein activity supports a functional role for dynein in the metaphase checkpoint pathway. Further evidence for such a role can be seen in the behaviour of dynein at the kinetochore in response to drugs that alter microtubule assembly and dynamics within wild-type neuroblasts. In a manner similar to that of known checkpoint proteins — Rod (ref. 28), Zw10 (ref. 29), Bub1 (ref. 30), Mad2 (ref. 31) — dynein strongly accumulates at the kinetochores of metaphase neuroblasts treated with either the microtubule-destabilizing drug colchicine or the microtubule-stabilizing drug Taxol (Fig. 6).

Dynein mutant neuroblasts are delayed in metaphase by activating the metaphase checkpoint. Hypomorphic dynein mutant (*Dhc64C*$^{6-10}$*/Df(3L)10H*) animals survive and develop until pharate adulthood, and their mitotic machinery exhibits a variety of mild defects. In addition to the mislocalization of Rod, the mutant cells occasionally display various degrees of defects in spindle assembly and in centrosome attachment or positioning (Figs 7 and 8). These defects probably contribute to the occurrence of polyploid neuroblasts and the observed abnormal anaphase chromosome configurations (Fig. 7, polyploid metaphases in Table 1).

Several different assays indicate that the metaphase checkpoint is activated in the dynein mutant neuroblasts. First, both the mitotic index and the ratio of metaphase to anaphase cells are significantly elevated (Table 1) compared with wild-type. Both indexes are hallmarks of a block in the progression of mitosis past metaphase. Second, the *Dhc64C*$^{6-10}$ mutant neuroblasts display a normal response to treatment by the microtubule-depolymerizing drug colchicine. In wild-type cells treated with colchicine, cells accumulate in a prometaphase-like state, with the typical elevated cyclin B levels expected of prometaphase. It has been shown previously that colchicine-treated neuroblasts of metaphase checkpoint mutants *rod, zw10* or *bub1* do not accumulate in prometaphase, but instead display a high-frequency (30–50%) of precocious degradation of cyclin B (ref. 21), and premature sister chromatid separation (PSCS), indicating an exit from the mitotic state. However, in colchicine-treated mutant dynein *Dhc64C*$^{6-10}$*/Df(3L)10H* neuroblasts, cells with condensed chromosomes accumulated and (see Supplementary Information, Fig. S1, arrows) consistently exhibited high levels of cyclin B, and essentially no PSCS (Table 1). Therefore, neuroblasts containing mutant dynein, in which Rod is inherently unable to move off kinetochores, experience a checkpoint-induced delay in the metaphase–anaphase transition in both the presence and the absence of colchicine. This delay is sensitive to perturbations of the checkpoint, because animals that are doubly mutant for *Dhc* and *rod* do not exhibit a metaphase block and resemble the *rod* loss-of-function phenotype alone (Table 1). This result confirms that the metaphase block of the dynein mutant neuroblasts is due to the activation of the metaphase checkpoint.

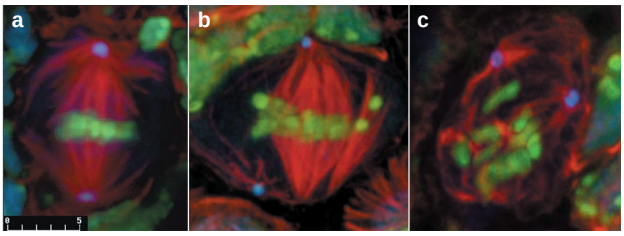

Figure 8 **Dynein mutants exhibit defects in spindle assembly that might affect chromosome behaviour and checkpoint controls.** A range of spindle defects are seen in the dynein mutant neuroblasts. **a**, Confocal image of a metaphase wild-type third-instar neuroblast immunostained to show tubulin (red), DNA (green) and centrosome antigen CP190 (blue). **b**, **c**, Two examples of spindle defects seen in dynein mutant neuroblasts (**a**) with a moderately frayed spindle with detached pole (**b**) and a severely disrupted metaphase array (**c**).

Discussion

Our visualization of Dmn–GFP during mitotic divisions in the *Drosophila* embryo provides new information on the likely sites of action for the dynein–dynactin complex during mitosis. Most significantly, we show here that Dmn–GFP first accumulates at kinetochores upon breakdown of the nuclear envelope, reaches peak levels in early prometaphase and subsequently translocates to spindle poles; it is thereby depleted from metaphase kinetochores. The polewards translocation of Dmn–GFP off kinetochores and towards their associated spindle poles coincides with the attachment and congression of chromosomes to the metaphase plate.

The dynamics of Dmn–GFP during mitosis probably provide a reliable indicator of both dynein and dynactin distribution. We demonstrate that the Dmn–GFP product is incorporated into the dynactin complex, does not disrupt dynactin assembly and causes no obvious detrimental consequence to viability. The functionality of Dmn–GFP transgene is confirmed by observations that the transgene can rescue mutant alleles of the *Drosophila* p50 gene (E. Wojcik and T. Hays, unpublished observations). The close association between the dynein and dynactin complexes is well known, and recent evidence predicts a similar polewards transport of dynein from the kinetochores of meiotic grasshopper chromosomes[22]. Dmn–GFP also displays patterns of localization that support previously postulated roles for dynein in the establishment and maintenance of the mitotic apparatus.

The observed dynamic loss of Dmn–GFP from kinetochores is similar to the depletion of kinetochore-associated checkpoint proteins seen during the progression of prometaphase (see, for example, ref. 32). A striking finding in our studies is that the distribution of the kinetochore checkpoint protein, Rod, is dependent on dynein motor function. In a strong dynein mutant the polewards transport of Rod complex off prometaphase kinetochores and along the spindle microtubules is blocked. Instead, Rod localizes and accumulates with the mutant dynein protein, which itself remains concentrated at kinetochores. This is in marked contrast to the substantial depletion of dynein from metaphase kinetochores in wild-type cells (Fig. 5a, see also ref. 22).

Despite the disruption in Rod behaviour, dynein dysfunction does not impair the activation of the metaphase checkpoint. *Dhc64C*$^{6-10}$ cells display an elevated mitotic index, with few anaphases (Table 1). However, the spindle defects are relatively mild in *Dhc64C*$^{6-10}$, with chromosomes often correctly congressed on a metaphase plate (see Fig. 3, for example). In contrast to the Dhc mutant, previous work has shown that the Rod-null mutations result in a failure to activate or maintain the metaphase checkpoint[21]. Furthermore, as with activation of the checkpoint in the presence of microtubule inhibitors, the metaphase delay evident in dynein mutant neuroblasts is eliminated by loss-of-function mutations in *rod*. This result confirms that the metaphase delay that occurs in the dynein mutant is caused by the activated metaphase checkpoint.

Why is the checkpoint activated in *Dhc64C*$^{6-10}$cells? It is not completely clear what physical events are being monitored by the checkpoint system reviewed in refs 24, 33). One class of models predicts that activation of the checkpoint does not require dynein but is instead a response to dynein dysfunction, either at the kinetochore or perhaps elsewhere during spindle morphogenesis. One explanation for the elevated mitotic index in the *Dhc64C*$^{6-10}$ mutants is therefore that the defective dynein encoded by *Dhc64C*$^{6-10}$ causes subtle changes in the kinetochore–microtubule linkages and that these are detected by the metaphase checkpoint apparatus as 'improperly attached' chromosomes. Alternatively, kinetochore dynein could act to produce tension that in turn somehow activates the polewards transport of Rod transport. For example, the dynein-mediated activation of a second motor could explain the dependence of Rod distribution on dynein; however, it does not readily account for the observed localization of Rod with both wild-type and mutant dynein throughout mitosis. Taken together with the previously reported physical interaction between dynactin and the checkpoint apparatus[19], we believe that our results are most simply explained by the direct participation of dynein in the transport of the Rod complex.

We favour a more provocative interpretation of the data and suggest that dynein functions to shut off the metaphase checkpoint apparatus. In this model we envisage the metaphase checkpoint pathway in one of two states, active or inactive. Rod and Zw10 function to initiate and/or maintain the metaphase checkpoint in the active state, whereas dynein functions in this pathway to inactivate the checkpoint. In this way, dynein has a key role in the metaphase checkpoint that is independent of the role of proteins known to maintain the checkpoint. Importantly, this model successfully predicts many of our observations such as the prolonged metaphase delay in the dynein mutants and the suppression of this phenotype by Rod loss-of-function mutants. In keeping with existing models of checkpoint activation, it follows that the active checkpoint apparatus, including the Rod–Zw10 complex, functions only when assembled on the kinetochore[32]. We propose that a principal route of checkpoint inactivation is by the dynein-mediated removal of the Rod–Zw10 complex from the kinetochore. Recently, a similar polewards transport of other checkpoint proteins (Mad2, 3F3, and BubR1) off mammalian kinetochores has also been shown to depend directly on dynein and dynactin function (B. J. Howell, J. C. Canman, B. F. McEwen, D. B. Hoffman, G. Cassels and E. D. Salmon, personal communication). These authors have invoked a similar model that implicates dynein-based transport of kinetochore checkpoint proteins in a mechanism that acts to turn off the activated checkpoint.

The parallel behaviours of Rod–Zw10 and checkpoint components Mad2, 3F3 and BubR1 suggest that they might form a single complex whose polewards streaming and inactivation are mediated by dynein. To substantiate the proposed direct role for dynein in the modulation of checkpoint activity, further experiments are required. In particular, we need definitively to establish the physical interactions between dynein, checkpoint components and kinetochores. Moreover, an understanding is needed of how dynein association with the kinetochore might be regulated by microtubule attachment and the production of tension[22]. Our studies reveal that a fraction of the kinetochore dynein remains localized at the kinetochore throughout mitosis. It will be important to determine whether this fraction mediates polewards chromosome movement[15–18]. □

Methods

Cytological analysis of mitosis in *Drosophila* by phase-contrast light microscopy and immunofluorescence.

The *Drosophila* stocks used in this study, including all the dynein alleles, have been described previously[34]. Dynein mutant third-instar larvae were identified by the segregation of the larval genetic marker *Tubby* (*Tb*). Orcein-stained chromosome spreads from third-instar larval brains were prepared as described[35]. Photographic images of the chromosome spreads were obtained with a Zeiss Axioskop. Images were digitized with a Polaroid Sprintscan 35 slide scanner and prepared for printing with Adobe Photoshop.

Time-lapse recording of Dmn–GFP in living embryos.

Drosophila p50/Dmn–GFP was constructed from genomic DNA fragments isolated by polymerase chain reaction (PCR) and subcloned into pCaSpeR4 for germline transformation. The transgene construct contains 2,491 base pairs (bp) of promoter/enhancer sequence and 419 bp 3′ of the putative polyadenylation signal, in addition to the *Dmn* transcribed region. A GFP open reading frame was subcloned into this genomic context by PCR, to result in C-terminal fusion to the *Dmn* translated sequence, leaving the entire native *Dmn* coding sequence intact. None of the homozygous insertion lines suffered from reduced viability. In parallel, ~500 embryos each were collected from the wild-type and homozygous insertion stocks and the number of embryos that were unhatched 30 h after collection was determined (wild type, 37/550; *Dmn–GFP*, 45/520). The hatching frequency for wild-type embryos was normalized to 100% and the relative frequency for Dmn–GFP embryos was calculated as 98% of the wild type. Transgenic embryos were prepared for image acquisition by dechorionation and protected from desiccation by a layer of halocarbon oil. All images were collected on a Leica TCS SP confocal microscope. Time-lapse recording intervals ranged between 3 and 10 s between frames. Image stacks were converted to QuickTime format and video clips were produced with Final Cut Pro (Apple Computer).

Characterization of Dmn–GFP incorporation into the dynactin complex.

Soluble extracts of ovaries from Dmn–GFP and wild-type flies were sedimented through 5–20% sucrose gradients made in PMEG buffer (100 mM PIPES pH 6.9, 5 mM magnesium acetate, 5 mM EGTA, 0.1 mM EDTA, 0.5 mM dithiothreitol, 0.9 M glycerol; with protease inhibitors 10 μg ml^{-1} aprotinin, 1 μg ml^{-1} leupeptin, 1 μg ml^{-1} pepstatin, 0.1 μg ml^{-1} soybean trypsin inhibitor, 0.1 μg ml^{-1} *p*-toluene-sulphonyl-L-arginine methyl ester, 0.1 μg ml^{-1} benzamidine). Total protein (2 mg) in 300 μl volume was layered on 11.2-ml gradients, which were centrifuged at 230,000*g* for 16 h at 4 °C, then collected into 0.5-ml fractions. Sedimentation standards cytochrome *c*, catalase and thyroglobulin were run in parallel on a separate gradient.

Equal volumes of each fraction were analysed by SDS–PAGE and immunoblotting; 5–10% gradient gels made with 1% bisacrylamide were blotted to poly(vinylidene difluoride) membrane and processed with a chemiluminescent detection method (Applied Biosystems). Blots were probed with a monoclonal antibody against the fly dynein heavy chain P1H4 (ref. 12), a polyclonal serum TE2 raised against the fly dynactin subunit p150 (ref. 36) and a monoclonal anti–GFP antibody (generously provided by M. Titus). The sedimentation profiles observed for the dynein and dynactin complexes are similar to those described previously[37].

Cytological analysis of mitosis in *Drosophila* giant neuroblasts by epifluorescence and confocal microscopy.

Third-instar wild-type and mutant (*Dhc*$^{e-10}$*/Df(3L)10H*) brains were isolated and prepared in parallel by using a procedure described previously[35], with the following modifications. Microtubule arrays were preserved with a fixation protocol that does not require Taxol to prevent inadvertent depolymerization: excised brains were transferred to fixative (10% formaldehyde, PBS, 2 mM $MgCl_2$, 1 mM EGTA pH 7.5) for 30 min. The fixed tissue was permeabilized for 10 min in 0.3% Tween 20, 0.3% saponin, 2% dimethylsulphoxide (DMSO) in PBS and incubated in blocking buffer (1% BSA, 5% glycerol, 5% goat serum, 0.45% cold-water fish gelatin, 5% DMSO, 0.1% Tween 20, PBS pH 7.2). Tubulin was labelled with monoclonal mouse anti-(tubulin) (DM1A; Sigma) diluted 1:200 in blocking buffer and Texas-red-conjugated goat anti-mouse secondary antibody (Jackson, Immunoresearch Labs, West Grove, Pennsylvania) diluted 1:200. Cytoplasmic dynein was detected with affinity-purified *Drosophila* dynein peptide antibody P1H4 at 1:500 dilution[12]. Centrosomes were labelled with rabbit anti-CP190 (provided by W. Whitfield, University of Dundee, Scotland) at a dilution of 1:250 and Cy-5 goat anti-rabbit (Amersham, Arlington Heights, Illinois) diluted 1:200. DNA was revealed with Oligreen dye (Molecular Probes).

Over 25 mutant and wild-type brains were examined systematically, in several separate experiments, for mitotic cells in which all three probes were simultaneously visible. Each brain yielded approximately 10–15 metaphase neuroblasts at depths within the tissue that were accessible to confocal imaging.

Drug treatments with either 5 μm Taxol, or 1 μg ml^{-1} colchicine, were performed on dissected third-instar larval brains by using established protocols[38], with the following modifications. Larvae were dissected in Schneider's medium at 25 °C. Brains were incubated for 2 h at 25 °C in Schneider's solution containing either drug and then fixed and prepared for immunofluorescence as above. For PSCS analysis, third-instar larvae brains were dissected in 0.7% NaCl, cultured for 1 h in 100 mM colchicine in 0.7% NaCl, then transferred individually to 1% sodium citrate hypotonic solution for exactly 5 min before being squashed in aceto-orecein, as described in ref. 21.

Confocal images were collected with a Bio-Rad MRC 1024 scanning confocal system mounted on a Nikon Diaphot 300 microscope equipped with a 15 mW krypton–argon laser. A Nikon 60×/1.4 numerical aperture Planapochromatic objective lens was used for all analyses. Image files were processed with Confocal Assistant (Todd Brejle) and/or ScionImage PC (Scion Corp.). Images were printed from Adobe Photoshop with a Fujix Pictrography 3000 colour printer.

For conventional immunofluorescence of Rod, dynein and tubulin, brains dissected from third-instar *Drosophila* larvae were prepared as described in ref. 19. Antibodies were used at the following dilutions: crude rabbit anti-Rod[28], 1/500; mouse anti dynein DM1A, 1/1,000; anti-dynein 1/500; Alexa 594 and 488 anti-mouse and anti-rabbit IgGs (Molecular Probes, Eugene, Oregon), 1/300. DNA was labelled with 4′,6-diamidino-2-phenylindole at 0.5 μg ml^{-1}. For staining with cyclin B, we used a rabbit anti-cyclin-B (a gift from C. Lehner) at 1:2,000 dilution. Preparations were viewed with a 63× objective with a Nikon Microphot microscope with phase contrast and epifluorescence. Images were collected with a Princeton Instruments cooled charge-coupled-device camera with Metamorph software.

RECEIVED 30 MAY 2001; REVISED 12 JULY 2001; ACCEPTED 17 AUGUST 2001; PUBLISHED 11 OCTOBER 2001.

1. Merdes, A., Heald, R., Samejima, K., Earnshaw, W. C. & Cleveland, D. W. Formation of spindle poles by Dynein/Dynactin-dependent transport of NuMA. *J. Cell Biol.* **149,** 851–862 (2000).
2. Robinson, J. T., Wojcik, E. J., Sanders, M. A., McGrail, M. & Hays, T. S. Cytoplasmic dynein is required for the nuclear attachment and migration of centrosomes during mitosis in *Drosophila*. *J. Cell Biol.* **146,** 597–608 (1999).
3. Purohit, A., Tynan, S. H., Vallee, R. & Doxsey, S. J. Direct interaction of pericentrin with cytoplasmic dynein light intermediate chain contributes to mitotic spindle organization. *J. Cell Biol.* **147,** 481–492 (1999).
4. Palazzo, R. E., Vaisberg, E. A., Weiss, D. G., Kuznetsov, S. A. & Steffen, W. Dynein is required for spindle assembly in cytoplasmic extracts of *Spisula solidissima* oocytes. *J. Cell Sci.* **112,** 1291–1302 (1999).
5. Heald, R. *et al.* Self-organization of microtubules into bipolar spindles around artificial chromosomes in *Xenopus* egg extracts. *Nature* **382,** 420–425 (1996).
6. Merdes, A., Ramyar, K., Vechio, J. D. & Cleveland, D. W. A complex of NuMA and cytoplasmic dynein is essential for mitotic spindle assembly. *Cell* **87,** 447–458 (1996).
7. Vaisberg, E. A., Koonce, M. P. & McIntosh, J. R. Cytoplasmic dynein plays a role in mammalian mitotic spindle formation. *J. Cell Biol.* **123,** 849–858 (1993).
8. O'Connell, C. B. & Wang, Y. L. Mammalian spindle orientation and position respond to changes in cell shape in a dynein-dependent fashion. *Mol. Biol. Cell* **11,** 1765–1774 (2000).
9. Heil-Chapdelaine, R. A., Tran, N. K. & Cooper, J. A. Dynein-dependent movements of the mitotic spindle in *Saccharomyces cerevisiae* do not require filamentous actin. *Mol. Biol. Cell* **11,** 863–872 (2000).
10. Adames, N. R. & Cooper, J. A. Microtubule interactions with the cell cortex causing nuclear movements in *Saccharomyces cerevisiae*. *J. Cell Biol.* **149,** 863–874 (2000).
11. Gonczy, P., Pichler, S., Kirkham, M. & Hyman, A. A. Cytoplasmic dynein is required for distinct aspects of MTOC positioning, including centrosome separation, in the one cell stage *Caenorhabditis elegans* embryo. *J. Cell Biol.* **147,** 135–150 (1999).
12. McGrail, M. & Hays, T. S. The microtubule motor cytoplasmic dynein is required for spindle orientation during germline cell divisions and oocyte differentiation in *Drosophila*. *Development* **124,** 2409–2419 (1997).
13. Li, Y. Y., Yeh, E., Hays, T. & Bloom, K. Disruption of mitotic spindle orientation in a yeast dynein mutant. *Proc. Natl Acad. Sci. USA* **90,** 10096–10100 (1993).
14. Carminati, J. L. & Stearns, T. Microtubules orient the mitotic spindle in yeast through dynein-dependent interactions with the cell cortex. *J. Cell Biol.* **138,** 629–641 (1997).
15. Steuer, E. R., Wordeman, L., Schroer, T. A. & Sheetz, M. P. Localization of cytoplasmic dynein to mitotic spindles and kinetochores. *Nature* **345,** 266–268 (1990).
16. Pfarr, C. M. *et al.* Cytoplasmic dynein is localized to kinetochores during mitosis. *Nature* **345,** 263–265 (1990).
17. Sharp, D. J., Rogers, G. C. & Scholey, J. M. Cytoplasmic dynein is required for poleward chromosome movement during mitosis in *Drosophila* embryos. *Nature Cell Biol.* **2,** 922–930 (2000).
18. Savoian, M. S., Goldberg, M. L. & Rieder, C. L. The rate of poleward chromosome motion is attenuated in *Drosophila zw10* and *rod* mutants. *Nature Cell Biol.* **2,** 948–952 (2000).
19. Starr, D. A., Williams, B. C., Hays, T. S. & Goldberg, M. L. ZW10 helps recruit dynactin and dynein to the kinetochore. *J. Cell Biol.* **142,** 763–774 (1998).
20. Chan, G. K., Jablonski, S. A., Starr, D. A., Goldberg, M. L. & Yen, T. J. Human Zw10 and ROD are mitotic checkpoint proteins that bind to kinetochores. *Nature Cell Biol.* **2,** 944–947 (2000).
21. Basto, R., Gomes, R. & Karess, R. E. Rough deal and Zw10 are required for the metaphase checkpoint in *Drosophila*. *Nature Cell Biol.* **2,** 939–943 (2000).
22. King, J. M., Hays, T. S. & Nicklas, R. B. Dynein is a transient kinetochore component whose binding is regulated by microtubule attachment, not tension. *J. Cell Biol.* **151,** 739–748 (2000).
23. Banks, J. D. & Heald, R. Chromosome movement: Dynein-out at the kinetochore. *Curr. Biol.* 11, R128–R131 (2001).
24. Shah, J. V. & Cleveland, D. W. Waiting for anaphase: Mad2 and the spindle assembly checkpoint. *Cell* **103,** 997–1000 (2000).
25. Echeverri, C. J., Paschal, B. M., Vaughan, K. T. & Vallee, R. B. Molecular characterization of the 50-kD subunit of dynactin reveals function for the complex in chromosome alignment and spindle organization during mitosis. *J. Cell Biol.* **132,** 617–633 (1996).
26. Karki, S. & Holzbaur, E. L. Cytoplasmic dynein and dynactin in cell division and intracellular transport. *Curr. Opin. Cell Biol.* **11,** 45–53 (1999).
27. Scaërou, F. *et al.* The ZW10 and Rough Deal checkpoint proteins function together in a large, evolutionarily conserved complex targeted to the kinetochore. *J. Cell Sci.* (in the press).
28. Scaërou, F. *et al.* The rough deal protein is a new kinetochore component required for accurate chromosome segregation in *Drosophila*. *J. Cell Sci.* **112,** 3757–3768 (1999).
29. Williams, B. C., Gatti, M. & Goldberg, M. L. Bipolar spindle attachments affect redistributions of ZW10, a *Drosophila* centromere/kinetochore component required for accurate chromosome segregation. *J. Cell Biol.* **134,** 1127–1140 (1996).
30. Basu, J. *et al.* Mutations in the essential spindle checkpoint gene *bub1* cause chromosome missegregation and fail to block apoptosis in *Drosophila*. *J. Cell Biol.* **146,** 13–28 (1999).
31. Howell, B. J., Hoffman, D. B., Fang, G., Murray, A. W. & Salmon, E. D. Visualization of Mad2 dynamics at kinetochores, along spindle fibers, and at spindle poles in living cells. *J. Cell Biol.* **150,** 1233–1250 (2000).
32. Gorbsky, G. J., Chen, R. H. & Murray, A. W. Microinjection of antibody to Mad2 protein into mammalian cells in mitosis induces premature anaphase. *J. Cell Biol.* **141,** 1193–1205 (1998).
33. Gardner, R. D. & Burke, D. J. The spindle checkpoint: two transitions, two pathways. *Trends Cell Biol.* **10,** 154–158 (2000).
34. Gepner, J. *et al.* Cytoplasmic dynein function is essential in *Drosophila melanogaster*. *Genetics* **142,** 865–878 (1996).
35. Gonzalez, C. & Glover, D. M. in *The Cell Cycle: A Practical Approach* (eds Fantes, P. & Brooks, R.) 143–175 (IRL, Oxford, 1994).
36. Waterman-Storer, C. M. & Holzbaur, E. L. The product of the *Drosophila* gene, *Glued*, is the func-

tional homologue of the p150Glued component of the vertebrate dynactin complex. *J. Biol. Chem.* **271,** 1153–1159 (1996).
37. McGrail, M. *et al.* Regulation of cytoplasmic dynein function *in vivo* by the *Drosophila* Glued complex. *J. Cell Biol.* **131,** 411–425 (1995).
38. Theurkauf, W. E. & Heck, M. M. Identification and characterization of mitotic mutations in *Drosophila*. *Methods Cell Biol.* **61,** 317–346 (1999).

ACKNOWLEDGEMENTS
We acknowledge helpful discussions with all members of the Hays laboratory, and thank E. D. Salmon for communicating results before publication. This work was supported by grants to T.H. and E.W. from the National Institutes of Health (GM44757 and GM19123 respectively) and the American Heart Association (96002200). R.K., R.B. and F.S. performed this work at the UPR 2420 Centre de Génétique Moléculaire of the CNRS, associated with the Université Pierre et Marie Curie. R.K. was supported in part by grants from the CNRS and from the Association Pour la Recherche sur le Cancer (France). R.B. was supported by grants BD/11488/97 and P/BIA/111055/1998 from FCT, Portugal. F.S. was supported by Le Ministère Nationale de l'Enseignement Supérieur et de la Recherche.
Correspondence and requests for materials should be addressed to E.W. Supplementary information is available on *Nature Cell Biology*'s website (http://cellbio.nature.com).

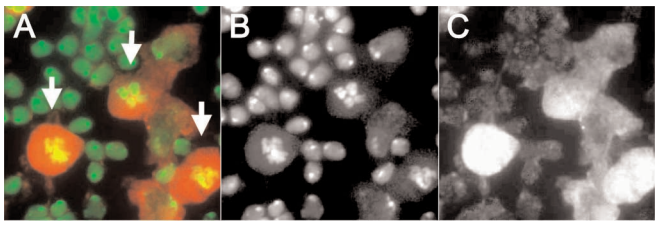

Figure S1 **Dynein mutant neuroblasts retain a checkpoint that prevents premature degradation of cyclin B.** In addition to a frequency of PSCS similar to wild-type (Table 1), the dynein mutant cells are able to delay cyclin B degradation when mitotic progression is blocked by the action of colchicine. Panel A shows a field of colchicine treated *Dhc64C*$^{6\text{-}10}$ mutant neuroblasts. Metaphase cells (arrows) consistently retain high levels of cyclin B. In A, DNA is green, and cyclin B is red. Cyclin B and DNA are also shown separately (Panels B and C, respectively).

Movie 1 **Time-lapse recordings of transformed syncytial were obtained by confocal microscopy, with 5 second intervals between frames.** We show here a typical recording of Dmn-GFP localization, showing one round of mitosis. Several interesting features are sequentially singled out and enlarged including; P50 localization at prometaphase, P50 enrichment in the cortex, and close up view of P50 streaming off metaphase kinetochores.